

Average-Cost Based Robust Structural Control

Nesbitt W. Hagood *
Massachusetts Institute of Technology
Cambridge, MA 02139

Abstract

A method is presented for the synthesis of robust controllers for linear time invariant structural systems with parameterized uncertainty. The method involves minimizing quantities related to the quadratic cost (\mathcal{H}_2 -norm) averaged over a set of systems described by real parameters such as natural frequencies and modal residues. Bounded average cost is shown to imply stability over the set of systems. Approximations for the exact average are derived and proposed as cost functionals. The properties of these approximate average cost functionals are established. The exact average and approximate average cost functionals are used to derive dynamic controllers which can provide stability robustness. The robustness properties of these controllers are demonstrated in illustrative numerical examples and tested in a simple SISO experiment on the MIT multi-point alignment testbed.

1 Introduction

The problems of stability and performance robustness in the presence of uncertain model parameters is of particular interest in the area of control of flexible structures. Uncertain stiffness, natural frequencies, damping, and actuator effectiveness all enter the model as variable parameters in the system matrices. The present work will attempt to address the robustness issues for parameterized plants by examining the properties of the quadratic (\mathcal{H}_2) performance of the system averaged over the set of plants given by the parameterization.

In the past, the average cost of a finite set of systems has been used to design for robustness in the face of parametric uncertainty [1], high frequency uncertainty [2], or variable flight regimes [3]. The goal is to design controllers that stabilize each model in a finite collection of plant models. This problem is called the simultaneous stabilization problem and has been treated previously in Refs. [4,5]. The cost averaged over a finite set of plants has also been used to derive full state feedback [6] and dynamic output feedback [7] compensators using parameter optimization to determine fixed-form compensator gains.

The present paper considers a quadratic performance criterion (formulated as the \mathcal{H}_2 system norm) averaged over a continuously parameterized set of plants controlled by a single feedback compensator. The model set is thus based on a continuous rather than discrete parameterization. This type of parameterization avoids ad hoc selection of plants to be represented in the control design and well represents the type of uncertain parameter dependence common in flexible structures. Typically

* Assistant Professor, Department of Aeronautics and Astronautics, Rm. 33-313 Tel. (617) 253-2738.

an uncertain parameter is specified by a range rather than a finite number of possible values. In addition, by considering this type of uncertainty, a link can be established between bounded average cost and simultaneous stability over the set of systems. The necessary conditions for minimization of a quadratic cost averaged over a continuously parameterized set of systems were previously derived for the static output feedback case in Ref. [8], and are here extended to the case of dynamic output feedback.

In the first section of this paper, the continuously parameterized model set and properties of the exact average cost are established. It will be shown that bounded average cost implies stability over the model set. Since it is difficult to compute the exact average cost, two approximations to it will be presented in the next section. The first approximation is based on a perturbation expansion about the nominal solution, while the second is derived from an approximation commonly used in the field of wave propagation in random media. Their properties and computation will be addressed. The derivation of these approximations to the average cost is based on operator decomposition methods which are presented in Ref. [9, 10].

The second half of the paper concerns the design of controllers based on exact and approximate average cost minimization. The approach taken involves fixing the order of the compensator and optimizing over the feedback gains. This fixed-structure approach is a direct extension of the technique utilized in [6, 7, 11]. The controllers derived from the exact and approximate average minimization will be compared in numerical examples. In addition, an average-cost based controller will be compared to traditional LQG designs in an experimental application of the methods to control a precision optical path on the MIT multipoint alignment testbed.

2 The Average Cost

In the following sections, the average cost will be examined as a cost functional for control design. The first step in this process is to define the set of systems over which the quadratic cost (\mathcal{H}_2 -norm) of the system is averaged. The next step is to examine the average cost for properties which will be useful in the design of stabilizing compensators.

2.1 The General Set of Systems

The concept of the model set, a set of plants parameterized in terms of real parameters, will now be introduced. Throughout the rest of this work, the standard system notation in Ref. [12] will be used. The set \mathcal{G}_g of systems is parameterized as follows

$$\mathcal{G}_g = \{G_g(\alpha) \mid \forall \alpha \in \Omega\} \quad (1)$$

where $\Omega \in \mathbb{R}^r$ is a compact region over which a distribution function, $\mu(\alpha)$, is defined. Each system is described in the state space as

$$G_g(\alpha) = \left[\begin{array}{c|cc} A(\alpha) & B_1(\alpha) & B_2(\alpha) \\ \hline C_1(\alpha) & 0 & D_{12}(\alpha) \\ C_2(\alpha) & D_{21}(\alpha) & 0 \end{array} \right] \quad (2)$$

where $A(\alpha) \in \mathbb{R}^{n \times n}$, $B_2(\alpha) \in \mathbb{R}^{n \times m}$, $C_2(\alpha) \in \mathbb{R}^{l \times n}$, $B_1(\alpha) \in \mathbb{R}^{n \times p}$, $C_1(\alpha) \in \mathbb{R}^{q \times n}$, $\alpha \in \Omega$ and the D matrices are partitioned conformally.

In addition to the assumptions implicit in the set definition, the following assumptions will be made on the system.

- (i) For each $\alpha \in \Omega$, $(A(\alpha), B_1(\alpha))$ is stabilizable, $(C_1(\alpha), A(\alpha))$ is detectable.
- (ii) For each $\alpha \in \Omega$, $(A(\alpha), B_2(\alpha))$ is stabilizable, $(C_2(\alpha), A(\alpha))$ is detectable.
- (iii) $D_{12}^T(\alpha) \begin{bmatrix} C_1(\alpha) & D_{12}(\alpha) \end{bmatrix} = \begin{bmatrix} 0 & R(\alpha) \end{bmatrix}$, $R(\alpha) > 0 \forall \alpha \in \Omega$
- (iv) $D_{21}(\alpha) \begin{bmatrix} B_1^T(\alpha) & D_{21}^T(\alpha) \end{bmatrix} = \begin{bmatrix} 0 & V(\alpha) \end{bmatrix}$, $V(\alpha) > 0 \forall \alpha \in \Omega$
- (v) The set of systems, \mathcal{G}_g , must be simultaneously stabilizable. The conditions for simultaneously stabilizable sets of systems have been considered in Ref. [4, 5].

Assumptions (i) and (ii) are made to ensure the observability and controllability of unstable modes from the controller and the disturbability and measurability of the unstable modes in the performance. Assumption (iii) implies that $C_1 x$ and $D_{12} u$ are orthogonal so that there is no cross weighting between the output and control. R is positive definite so that the weighting on z includes a nonsingular weighting on the control. Assumption (iv) is dual to (iii) and ensures the noncorrelation of the plant and sensor noise. It is equivalent to the standard conditions assumed for the Kalman filter. Assumption (v) is made to guarantee existence of the controllers derived in the next section.

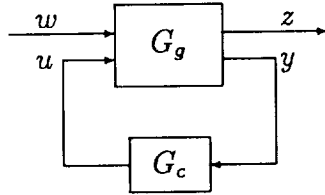


Figure 1: The Control Problem for Dynamic Output Feedback

It is useful at this point to consider the set of closed-loop systems. The control problem for each element of the model set can be illustrated by the standard block diagram shown in Figure 1. Given the set \mathcal{G}_g of open loop systems and the compensator of order, n_c , with

$$G_c = \left[\begin{array}{c|c} A_c & B_c \\ \hline C_c & 0 \end{array} \right] \quad (3)$$

with input y and output u , the set of closed-loop transfer functions from w to z , \mathcal{G}_{zw} , can be defined. Each element of \mathcal{G}_{zw} can be expressed in state space form for dynamic output feedback as:

$$\begin{aligned} G_{zw}(\alpha) &= \left[\begin{array}{cc|c} A(\alpha) & B_2(\alpha)C_c & B_1(\alpha) \\ B_c C_2(\alpha) & A_c & B_c D_{21}(\alpha) \\ \hline C_1(\alpha) & D_{12}(\alpha)C_c & 0 \end{array} \right] \\ &= \left[\begin{array}{c|c} \tilde{A}(\alpha) & \tilde{B}(\alpha) \\ \hline \tilde{C}(\alpha) & 0 \end{array} \right] \end{aligned} \quad (4)$$

where $\tilde{A}(\alpha) \in \mathbb{R}^{\tilde{n} \times \tilde{n}}$, $\tilde{B}(\alpha) \in \mathbb{R}^{\tilde{n} \times p}$, $\tilde{C}(\alpha) \in \mathbb{R}^{q \times \tilde{n}}$ are the closed-loop system matrices of order $\tilde{n} = n + n_c$.

2.2 The Average \mathcal{H}_2 -norm as a Cost Functional

Having defined a parameterized set of systems, it is now possible to define a cost which will reflect the system parameter uncertainty. One possible approach is to look at the quadratic cost (system

\mathcal{H}_2 -norm) averaged over set of possible systems. In this section this average cost will be defined and discussed in the context of computing the average performance of a linear time invariant system. We will start by considering the definition and properties of the exact average cost. The exact average cost is defined as the closed-loop system \mathcal{H}_2 -norm averaged (integrated) over the model set.

$$J(G_c) = \int_{\Omega} \|G_{zw}(\alpha)\|_2^2 d\mu(\alpha) = \langle \|G_{zw}(\alpha)\|_2^2 \rangle \quad (5)$$

where $\int_{\Omega} \cdot d\mu(\alpha) = \langle \cdot \rangle$ is the averaging function.

The first property of interest is the relationship between simultaneous stability and bounded average \mathcal{H}_2 -norm. If the exact averaged cost, Eq. (5), over the set \mathcal{G}_{zw} is bounded

$$J(G_c) = \langle \|G_{zw}(\alpha)\|_2^2 \rangle < \infty \quad (6)$$

then all the parameterized closed-loop systems, $G_{zw}(\alpha)$, are asymptotically stable except for the possibility of having an isolated plant in the set with poles on the imaginary axis. In general, no system in \mathcal{G}_{zw} can have eigenvalues with positive real parts.

This result provides the motivation for examining the average cost since controllers designed by minimizing the average cost will be guaranteed stable over the model set. Since at each value of α the cost is given by the solution of a Lyapunov equation, the next step in the development is to relate the averaged \mathcal{H}_2 -norm to the averaged solution of a parameterized Lyapunov equation. This gives a possible method of calculating the average cost by calculating the average solution to a linear Lyapunov equation.

Given a specified compensator, G_c , if the parameterized closed-loop systems, $G_{zw}(\alpha)$, are stable for almost all $\alpha \in \Omega$ then

$$J(G_c) = \text{tr} \left\{ \left\langle \tilde{Q}(\alpha) \tilde{C}^T(\alpha) \tilde{C}(\alpha) \right\rangle \right\} \quad (7)$$

where for each $\alpha \in \Omega$, $\tilde{Q}(\alpha)$ is the unique positive definite solution to

$$0 = \tilde{A}(\alpha) \tilde{Q}(\alpha) + \tilde{Q}(\alpha) \tilde{A}^T(\alpha) + \tilde{B}(\alpha) \tilde{B}^T(\alpha) \quad (8)$$

The exact averaged cost is difficult to calculate because of the difficulty of averaging the solution to the Lyapunov equation, Eq. (8). In most instances the solution to Eq. (8) can be obtained explicitly as a function of α , and then averaged either numerically or symbolically. There are also numerous numerical techniques for approximating the average solution such as a Monte-Carlo or direct numerical integration. The computational issues will be discussed in a latter section.

3 Approximate Average Costs

In this section, explicit equations for the calculation of approximate average costs will be derived. Two types of approximations will be discussed. The first is derived from a truncation of the perturbation expansion of the solution of the parameterized Lyapunov equation, Eq. (8), about the nominal solution. The second is a more sophisticated approximation for the solution of parameterized linear operators which has been widely used in the fields of wave propagation in random media [13], and turbulence modelling. A brief presentation of the relevant work in parameterized linear operators is presented in Appendix A of reference 10.

3.1 The Structured Set of Systems

It will prove useful to define a different set of systems with more restrictive assumptions on the functional form of the parameter dependence of the system matrices. The first assumption is that only parameter uncertainties entering into the closed-loop \tilde{A} matrix will be considered. This amounts to restricting the \tilde{B} and \tilde{C} matrices to being parameter independent. This assumption is not overly restrictive for stability robustness considerations since only uncertainties in the closed-loop A matrix affect stability. The uncertainties in the \tilde{B} and \tilde{C} matrices would however affect average performance. This uncertainty restriction is made primarily to enable derivation of approximations to the average cost.

The general uncertain set of systems in (2) can be specialized to a more structured set which allows less general parameter dependence. The structured set, Ω_s , of parameter vectors, α , is defined

$$\Omega = \left\{ \alpha : \alpha \in \mathbb{R}^r, \delta_i^L \leq \alpha_i \leq \delta_i^U \quad i = 1, \dots, r \right\} \quad (9)$$

where δ_i^L and δ_i^U are the lower and upper bounds for the i^{th} uncertain parameter. In addition, the parameter dependence of the elements of the remaining matrices will be assumed to be linear functions of the parameters. This is a very restrictive assumption but necessary if computable approximations for the average are to be derived. If they are in fact not linear functions, then the matrices must be linearized about the nominal values of the parameters.

Once the parameter dependence has been made linear a more structured set, \mathcal{G}_s , of systems can be defined

$$\mathcal{G}_s = \{G_s(\alpha) : \alpha \in \Omega_s\} \quad (10)$$

where Ω_s is the structured set of parameter vectors and each element of \mathcal{G}_s is described in the state space as

$$G_s(\alpha) = \left[\begin{array}{c|cc} A_0 + \sum_{i=1}^r \alpha_i A_i & B_1 & B_{2_0} + \sum_{i=1}^r \alpha_i B_{2_i} \\ \hline C_1 & 0 & D_{12} \\ \hline C_{2_0} + \sum_{i=1}^r \alpha_i C_{2_i} & D_{21} & 0 \end{array} \right] \quad (11)$$

where for $i = 0, \dots, r$; $A_i \in \mathbb{R}^{n \times n}$, $B_{2_i} \in \mathbb{R}^{n \times m}$, $C_{2_i} \in \mathbb{R}^{l \times n}$, and $B_1 \in \mathbb{R}^{n \times p}$, $C_1 \in \mathbb{R}^{q \times n}$.

Just as for the general set of systems, a set of closed-loop transfer functions, denoted \mathcal{G}_{zw} , can be generated using the structured set of systems. This closed-loop set can be expressed in state space form for dynamic output feedback as

$$\begin{aligned} G_{zw}(\alpha) &= \left[\begin{array}{cc|c} A_0 + \sum_{i=1}^r \alpha_i A_i & B_{2_0} C_c + \sum_{i=1}^r \alpha_i B_{2_i} C_c & B_1 \\ B_c C_{2_0} + \sum_{i=1}^r \alpha_i B_c C_{2_i} & A_c & B_c D_{21} \\ \hline C_1 & D_{12} C_c & 0 \end{array} \right] \\ &= \left[\begin{array}{c|c} \tilde{A}_0 + \sum_{i=1}^r \alpha_i \tilde{A}_i & \tilde{B} \\ \hline \tilde{C} & 0 \end{array} \right] \end{aligned} \quad (12)$$

Because of the form assumed for the uncertainty, only the resulting closed-loop A matrix, $\tilde{A}(\alpha) \in \mathbb{R}^{\tilde{n} \times \tilde{n}}$, is parameter dependent and the closed-loop system is strictly proper.

3.2 Perturbation Expansion Approximation

At this point, we can begin our exposition on the perturbation expansion approximation to the exact average cost. Given a specified compensator, G_c , the perturbation approximation to the exact average cost is given by:

$$J^P(G_c) = \text{tr} \left\{ (\tilde{Q}^0 + \tilde{Q}^P) \tilde{C}^T \tilde{C} \right\} \quad (13)$$

where the nominal cost, \tilde{Q}^0 , and the parameter dependent cost, \tilde{Q}^P , are the unique positive definite solutions to the following system of Lyapunov equations

$$0 = \tilde{A}_0 \tilde{Q}^0 + \tilde{Q}^0 \tilde{A}_0^T + \tilde{B} \tilde{B}^T \quad (14)$$

$$0 = \tilde{A}_0 \tilde{Q}^i + \tilde{Q}^i \tilde{A}_0^T + \sigma_i \left(\tilde{A}_i \tilde{Q}^0 + \tilde{Q}^0 \tilde{A}_i^T \right) \quad i = 1, \dots, r \quad (15)$$

$$0 = \tilde{A}_0 \tilde{Q}^P + \tilde{Q}^P \tilde{A}_0^T + \sum_{i=1}^r \sigma_i \left(\tilde{A}_i \tilde{Q}^i + \tilde{Q}^i \tilde{A}_i^T \right) \quad (16)$$

where σ_i is defined

$$\sigma_i^2 = \langle \alpha_i^2 \rangle \quad (17)$$

A detailed derivation of the perturbation expansion approximation is available in Ref. [9]. It is interesting to note that the system of Lyapunov equations presented in Eqs. (14-16) are coupled hierarchically. The nominal solution, \tilde{Q}^0 , can first be solved using Eq. (14) and the solution substituted into each of the i equations represented by Eq. (15). The solutions for these equations, \tilde{Q}^i , can then be used to solve for \tilde{Q}^P using Eq. (16).

The system of equations presented in Eqs. (14-16) are related to those inherent in the sensitivity system design methodology presented in Appendix A from Ref. [15]. This can be seen clearly by putting the equations for the component cost analysis in the notation used here.

$$0 = \tilde{A}_0 \tilde{Q}^0 + \tilde{Q}^0 \tilde{A}_0^T + \tilde{B} \tilde{B}^T \quad (18)$$

$$0 = \tilde{A}_0 \tilde{Q}^i + \tilde{Q}^i \tilde{A}_0^T + \sigma_i \left(\tilde{Q}^0 \tilde{A}_i^T \right) \quad i = 1, \dots, r \quad (19)$$

$$0 = \tilde{A}_0 \tilde{Q}^P + \tilde{Q}^P \tilde{A}_0^T + \sum_{i=1}^r \sigma_i \left(\tilde{A}_i \tilde{Q}^i + \tilde{Q}^i \tilde{A}_i^T \right) \quad (20)$$

Essentially there is only a single term omitted from (19) which is in (15).

This validates the assertion made in Ref. [15] that the sensitivity system cost is an approximation to the quadratic cost averaged over the uncertain parameters. The sensitivity system cost is essentially the average of the first three terms of a Taylor series expansion of the cost in powers of the uncertain parameters.

3.3 Bourret Approximation

An alternate approximation for the average cost can be derived based on series manipulation techniques presented in Refs. [9] and [14]. If the parameterized closed-loop systems, $G_{zw}(\alpha)$, are stable for almost all $\alpha \in \Omega$ then

$$J(G_c) \cong \text{tr} \left\{ \tilde{Q}^B \tilde{C}^T \tilde{C} \right\} \quad (21)$$

where \tilde{Q}^B is the unique positive definite solution to the following coupled system of Lyapunov equations

$$0 = \tilde{A}_0 \tilde{Q}^B + \tilde{Q}^B \tilde{A}_0^T + \tilde{B} \tilde{B}^T + \sum_{i=1}^r \sigma_i \left(\tilde{A}_i \tilde{Q}^i + \tilde{Q}^i \tilde{A}_i^T \right) \quad (22)$$

$$0 = \tilde{A}_0 \tilde{Q}^i + \tilde{Q}^i \tilde{A}_0^T + \sigma_i \left(\tilde{A}_i \tilde{Q}^B + \tilde{Q}^B \tilde{A}_i^T \right) \quad i = 1, \dots, r \quad (23)$$

where σ_i is defined from Eq. (17).

The system of Lyapunov equations presented in Eqs. (22-23) is very similar to the system generated by the perturbation expansion approximation. There is additional coupling occurring in Eq. (23). Instead of depending only on the nominal solution, \tilde{Q}^0 , these equations depend on the total Bourret approximate average solution, \tilde{Q}^B . This coupling complicates the solution procedure but leads to a more accurate approximation.

The system of Lyapunov equations represented by Eqs. (22-23) can be solved iteratively for the Bourret approximate average, \tilde{Q}^B , using the nominal solution, \tilde{Q}^0 , as the initial guess in Eq. (23). Equation (23) is then solved for \tilde{Q}^i which is used in Eq. (22) to obtain a new value for \tilde{Q}^B . Equations (22) and (23) can also be solved using Kronecker math techniques as described in Ref. [9].

These two approximations, the perturbation expansion and the Bourret, will be used to generate robustifying controllers in the sections to come. Because they are approximations, however, controllers derived using these approximations will not necessarily guarantee stability over the design set. Thus *a priori* guaranteed stability is sacrificed when using the approximations. The approximations are however much easier to calculate than the exact average cost, especially for systems with large numbers of uncertainties or high order. For such systems, the exact average cost is essentially uncomputable and the approximations must be used to derive controllers which increase robustness to parameter variations. These cost equations will now be used to develop parameter robust control strategies.

4 Dynamic Compensation

In this section three dynamic output feedback problems will be investigated. The first is the minimization of the exact average \mathcal{H}_2 -norm; the second is the minimization of the perturbation expansion approximation to the exact average; and the third is the minimization of the Bourret approximation to the exact average. The general technique will be to find the controller parameters which minimize quantities related to the exact average cost of the closed loop systems. This will be accomplished by first deriving necessary conditions of optimality and then using these in a numerical minimization scheme on the controller parameters. The derivations will begin with the exact average cost minimization since it is the basis of the approximation based cost minimization problems.

4.1 Exact Average Cost Minimization

In this section the formulation of the necessary conditions for the minimization of the exact average cost will be presented. The first step is to define the minimization problem for the exact average cost.

Problem 4.1 (Exact Average Cost Minimization Problem) *Given a set \mathcal{G}_g or \mathcal{G}_s of systems, determine the dynamic compensator or order, n_c ,*

$$G_c = \left[\begin{array}{c|c} A_c & B_c \\ \hline C_c & 0 \end{array} \right] \quad (24)$$

which minimizes the the closed-loop \mathcal{H}_2 -norm averaged over the model set.

$$J(G_c) = \langle \|G_{zw}(\alpha)\|_2^2 \rangle \quad (25)$$

In Section 2.2 the exact average cost was shown to be equivalent to

$$\mathcal{J}^E(G_c) = \text{tr} \left\{ \left\langle \tilde{Q}(\alpha) \tilde{C}^T(\alpha) \tilde{C}(\alpha) \right\rangle \right\} = J(G_c) \quad (26)$$

where $\tilde{Q}(\alpha)$ is given by the solution of

$$0 = \tilde{A}(\alpha) \tilde{Q}(\alpha) + \tilde{Q}(\alpha) \tilde{A}^T(\alpha) + \tilde{B}(\alpha) \tilde{B}^T(\alpha) \quad (27)$$

for each $\alpha \in \Omega$.

The first step in deriving necessary conditions is to append Eq. (27) to the cost using a parameter dependent, symmetric matrix of Lagrange multipliers, $\tilde{P}(\alpha) \in \mathbb{R}^{\tilde{n} \times \tilde{n}}$. The matrix of Lagrange multipliers must be parameter dependent because the appended equations are parameter dependent. The appended cost becomes

$$\begin{aligned} \mathcal{J}^E(G_c) = & \text{tr} \left\{ \left\langle \tilde{Q}(\alpha) \tilde{C}^T(\alpha) \tilde{C}(\alpha) \right\rangle \right\} \\ & + \text{tr} \left\{ \left\langle \left[\tilde{A}(\alpha) \tilde{Q}(\alpha) + \tilde{Q}(\alpha) \tilde{A}^T(\alpha) + \tilde{B}(\alpha) \tilde{B}^T(\alpha) \right] \tilde{P}(\alpha) \right\rangle \right\} \end{aligned} \quad (28)$$

where $\tilde{A}(\alpha)$, $\tilde{B}(\alpha)$, and $\tilde{C}(\alpha)$ are defined in Eq. (2). The necessary conditions for minimization of the exact average cost can now be stated by taking the derivatives with respect to G_c , $\tilde{P}(\alpha)$, and $\tilde{Q}(\alpha)$. An explanation of matrix derivatives can be found in Ref. [9] [16].

Suppose G_c , the dynamic compensator of order, n_c , defined in Eq. (24) solves the exact average cost minimization problem (4.1); then there exist matrices, $\tilde{Q}(\alpha)$ and $\tilde{P}(\alpha) \geq 0 \in \mathbb{R}^{\tilde{n} \times \tilde{n}}$ such that

$$0 = \langle \tilde{P}_{21}(\alpha) \tilde{Q}_{12}(\alpha) + \tilde{P}_{22}(\alpha) \tilde{Q}_{22}(\alpha) \rangle \quad (29)$$

$$\begin{aligned} 0 = & \langle \tilde{P}_{22}(\alpha) B_c D_{21}(\alpha) D_{21}^T(\alpha) \rangle \\ & + \langle \tilde{P}_{21}(\alpha) \tilde{Q}_{11}(\alpha) C_2^T(\alpha) + \tilde{P}_{22}(\alpha) \tilde{Q}_{21}(\alpha) C_2^T(\alpha) \rangle \end{aligned} \quad (30)$$

$$\begin{aligned} 0 = & \langle D_{12}^T(\alpha) D_{12}(\alpha) C_c \tilde{Q}_{22}(\alpha) \rangle \\ & + \langle B_2^T(\alpha) \tilde{P}_{11}(\alpha) \tilde{Q}_{12}(\alpha) + B_2^T(\alpha) \tilde{P}_{12}(\alpha) \tilde{Q}_{22}(\alpha) \rangle \end{aligned} \quad (31)$$

where $\tilde{Q}(\alpha)$ satisfies the parameterized Lyapunov equation

$$0 = \tilde{A}(\alpha) \tilde{Q}(\alpha) + \tilde{Q}(\alpha) \tilde{A}^T(\alpha) + \tilde{B}(\alpha) \tilde{B}^T(\alpha) \quad (32)$$

and $\tilde{P}(\alpha)$ satisfies the Adjoint Lyapunov equation

$$0 = \tilde{A}^T(\alpha) \tilde{P}(\alpha) + \tilde{P}(\alpha) \tilde{A}(\alpha) + \tilde{C}^T(\alpha) \tilde{C}(\alpha) \quad (33)$$

and $\tilde{Q}(\alpha)$ and $\tilde{P}(\alpha)$ are partitioned

$$\tilde{Q}(\alpha) = \begin{bmatrix} \tilde{Q}_{11}(\alpha) & \tilde{Q}_{12}(\alpha) \\ \tilde{Q}_{21}(\alpha) & \tilde{Q}_{22}(\alpha) \end{bmatrix}, \quad \tilde{P}(\alpha) = \begin{bmatrix} \tilde{P}_{11}(\alpha) & \tilde{P}_{12}(\alpha) \\ \tilde{P}_{21}(\alpha) & \tilde{P}_{22}(\alpha) \end{bmatrix} \quad (34)$$

with $\tilde{Q}_{11}, \tilde{P}_{11} \in \mathbb{R}^{n \times n}$, and $\tilde{Q}_{22}, \tilde{P}_{22} \in \mathbb{R}^{n_c \times n_c}$.

The result is a consequence of the differentiation of the cost, Eq. (28), with respect to $A_c, B_c, C_c, \tilde{P}(\alpha)$, and $\tilde{Q}(\alpha)$. Note that the necessary conditions that result from differentiation of the cost with respect to $\tilde{Q}(\alpha)$ and $\tilde{P}(\alpha)$, (32) and (33) respectively, are parameter dependent because $\tilde{Q}(\alpha)$ and $\tilde{P}(\alpha)$ are parameter dependent. The traditional LQG results are recovered in the case of no uncertainty and $n_c = n$.

The difficulty inherent in Eqs. (29)-(31) for the optimal gains is that they involve the average of the product of the solution of two parameter dependent Lyapunov equations, $\tilde{Q}(\alpha)$ and $\tilde{P}(\alpha)$. These matrices are only given as implicit functions of α in Equations (32) and (33). Only in the simplest of cases can the average of the product be solved for exactly. The solution can be obtained numerically by Monte-Carlo techniques, averaged numerically, or the explicit α dependence can be found by symbolic manipulations and the expressions averaged numerically or symbolically. All of these techniques are computationally intensive. In the next sections, the Perturbation Expansion approximation and Bourret approximation to the average cost will be minimized in an attempt to approximate the optimal solution by minimizing approximate but calculable expressions for the cost.

4.2 Approximate Average Cost Minimization

In this section the formulation of the necessary conditions for the minimization of the perturbation expansion approximate cost and the Bourret approximate cost will be discussed. The procedure is essentially the same as for the exact average cost only for the approximate costs the averages can be performed explicitly. The first step is to define the minimization problem. For the perturbation expansion approximation, the problem is to determine the dynamic compensator of order, n_c , defined in Eq. (24), which minimizes

$$\mathcal{J}^P(G_c) = \text{tr} \left\{ \left(\tilde{Q}^0 + \tilde{Q}^P \right) \tilde{C}^T \tilde{C} \right\} \quad (35)$$

where the nominal cost, \tilde{Q}^0 , and the parameter dependent cost, \tilde{Q}^P , are the unique positive definite solutions to the system of Lyapunov equations described in Eqs. (14)-(16).

As for the Exact Average, the first step in deriving the necessary conditions for the Minimization Problem is to append Eqs. (14)-(16) to the cost using parameter independent, symmetric matrices of Lagrange multipliers, \tilde{P}^0 , \tilde{P}^P , and \tilde{P}^i , $i = 1 \dots r \in \mathbb{R}^{2n \times 2n}$.

$$\mathcal{J}(G_c) = \text{tr} \left\{ \left(\tilde{Q}^0 + \tilde{Q}^P \right) \tilde{C}^T \tilde{C} \right\} \quad (36)$$

$$+ \text{tr} \left\{ \left[\tilde{A}_0 \tilde{Q}^0 + \tilde{Q}^0 \tilde{A}_0^T + \tilde{B} \tilde{B}^T \right] \tilde{P}^0 \right\} \quad (37)$$

$$+ \text{tr} \left\{ \sum_{i=1}^r \left[\tilde{A}_0 \tilde{Q}^i + \tilde{Q}^i \tilde{A}_0^T + \sigma_i \left(\tilde{A}_i \tilde{Q}^0 + \tilde{Q}^0 \tilde{A}_i^T \right) \right] \tilde{P}^i \right\} \quad (38)$$

$$+ \text{tr} \left\{ \left[\tilde{A}_0 \tilde{Q}^P + \tilde{Q}^P \tilde{A}_0^T + \sum_{i=1}^r \sigma_i \left(\tilde{A}_i \tilde{Q}^i + \tilde{Q}^i \tilde{A}_i^T \right) \right] \tilde{P}^P \right\} \quad (39)$$

where \tilde{A} , \tilde{B} , and \tilde{C} are defined in Eq. (12). Taking the derivatives with respect to $G_c, \tilde{P}^0, \tilde{P}^P, \tilde{P}^i$ and $\tilde{Q}^0, \tilde{Q}^P, \tilde{Q}^i$ gives the necessary conditions for minimization of the perturbation expansion approximation to the exact average cost. They can be found in Refs. [9] or [14]. The key difference

between these necessary conditions and those of the exact average cost minimization is that these equations are parameter independent (no longer parameterized) and thus easier to solve.

Similar to the perturbation expansion minimization, the problem for the Bourret approximate average cost compensator design is to determine the dynamic compensator of order, n_c , defined in Eq. (24), which minimizes

$$\mathcal{J}^B(G_c) = \text{tr} \left\{ \tilde{Q}^B \tilde{C}^T \tilde{C} \right\} \quad (40)$$

where \tilde{Q}^B is the unique positive definite solution to the system of coupled Lyapunov equations described in Eqs. (22)-(23).

As before, the first step in deriving the necessary condition is to append Eqs. (22) and (23) to the cost using parameter independent, symmetric matrices of Lagrange multipliers, \tilde{P}^B and \tilde{P}^i , $i = 1 \dots r \in \mathbb{R}^{\tilde{n} \times \tilde{n}}$. The equations have a form similar to (36). Taking the derivatives with respect to G_c , \tilde{P}^B , \tilde{P}^i and \tilde{Q}^B , \tilde{Q}^i gives the necessary conditions for minimization of the Bourret approximation to the exact average. They can be found in Refs. [9] or [14]. These necessary conditions are used for gradient information in a numerical minimization scheme described in the next section.

5 Controller Computation

In this section the techniques used to compute controllers based on the three cost functionals will be presented. The general technique used for computing the minimum cost controllers is parameter optimization. Since the controllers are fixed-form, the optimal controller can be found by minimizing the cost with respect to each of the parameters in the controller matrices. It should be noted that the parameter minimization is non-convex and the resulting minima can only be considered local minima although in practice they appear to be global. The gradient of the cost with respect to the controller parameters is given by the necessary conditions derived in Refs. [9] or [14]. These gradients are used in a standard Quasi-Newton numerical optimization routine to find the optimal controllers.

Since the minimizations are non-convex, the solution can be a function of the initial guess used in the optimization. This initial guess must also be a stabilizing compensator. This can be difficult to find for large values of uncertainty. These problems are overcome by first assuming little or no uncertainty and using the resulting controller as a starting point for calculating controllers at successively larger values of uncertainty. Standard LQG techniques can be used to find stabilizing compensators for systems with no uncertainty. The amount of uncertainty used in the design is gradually increased until the desired amount is reached. This solution technique is known as homotopic continuation. The general algorithm used to compute the controllers can be written.

- (i) **Initialize** the homotopy with a stabilizing compensator for the system with no uncertainty.
- (ii) **Increase** the amount of the uncertainty used in the design.
- (iii) **Minimize** the cost to derive a new compensator using a Broyden-Fletcher-Goldfarb-Shanno (BFGS) quasi-Newton scheme.
- (iv) **Evaluate** the resulting compensator to check the homotopy termination conditions.
- (v) **Iterate** on ii.

For dynamic full order compensation, the LQG compensator can be used. If the compensator is of reduced order, optimal projection or a heuristic compensator reduction procedure can be used to find stabilizing compensators. A small amount of uncertainty is then introduced into the problem

and a new controller is found by minimization starting from the initial guess. If the amount of uncertainty is increased too much in the step the initial guess will not be near the new optimal solution and may be difficult to locate. Taking too small of a step is computationally wasteful. If the compensator is optimal for a given amount of uncertainty, then the gradient is exactly zero since the necessary conditions are satisfied. As the uncertainty is increased, the previous optimal solution no longer satisfies the necessary conditions for the new problem and thus the magnitude of the gradient increases. A tolerance can be placed on how large the gradient is allowed to grow before the cost is reminimized. When the norm of the gradient exceeds the tolerance, the cost is reminimized to find a new compensator which satisfies the necessary conditions.

The minimization step is relatively straightforward. The appropriate cost is minimized with respect to the controller parameters using the necessary conditions for gradient information. The minimization technique used to derive the controllers presented in the next section was the popular BFGS quasi-Newton method with a modification to constrain the parameter minimization to the set of stabilizing compensators.

The computation of the cost and gradient is problem dependent. The cost is usually given by either the average value of a parameterized Lyapunov equation in the exact average case or by the solution of a set of coupled Lyapunov equations as for the approximation cost functionals. The gradient of the cost with respect to the compensator parameters is usually a function of the compensator parameters as well as the solution to a coupled set of Lyapunov equations.

The exact average cost is calculated by numerical integration over the parameter domain using a 32 point Gaussian quadrature. If more than three uncertain parameters must be retained in the design, then Monte-Carlo integration is the only feasible method of computing the averages needed for the cost and gradient calculations. The gradient functions also require averages of the product of the solutions of the parameterized Lyapunov equation and its adjoint. For speed, these averages can be computed at the same time as the average cost. The solution of the approximations functions are discussed in Refs. [9,10]. The perturbation expansion approximate average is computed by utilizing a standard Lyapunov solver and solving the equations hierarchically. The Bourret approximation is solved iteratively.

6 Numerical Examples

The three average-related cost functionals will be compared on some simple examples. To streamline discussion in these sections it is convenient to define a series of acronyms for the various designs.

EAM Exact Average Minimization

PEAM Perturbation Expansion Approximation Minimization

BAM Bourret Approximation Minimization

These acronyms will be used extensively in subsequent sections. It should be noted that the PEAM design is essentially equivalent the the sensitivity system cost minimization presented in [17]. To simplify discussion of the examples and compare with previous work, an LQG problem statement will be developed and shown to be equivalent to the system norm cost formalism.

6.1 LQG Problem Statement

To begin the comparison between the LQG problem statement and the system norm formalism, the system dynamics can be defined by

$$\dot{x}(t) = Ax(t) + Bu(t) + L\xi(t) \quad (41)$$

$$y(t) = Cx(t) + \theta(t) \quad (42)$$

where $x(t) \in \mathbb{R}^n$, $u(t) \in \mathbb{R}^m$, $y(t) \in \mathbb{R}^l$. The two noise input vectors, $\xi(t) \in \mathbb{R}^q$, the process noise, and $\theta(t) \in \mathbb{R}^p$, the sensor noise, are independent, zero mean, Gaussian white noise processes with constant intensity matrices, Ξ and Θ , respectively. The LQG cost functional which is to be minimized is defined by

$$J_{LQG} = E \left\{ \lim_{T \rightarrow \infty} \left(\frac{1}{T} \int_0^T x^T(t) Q x(t) + u^T(t) R u(t) dt \right) \right\} \quad (43)$$

which involves a positive semi-definite state weighting, $Q \in \mathbb{R}^{n \times n}$, and a positive definite control weighting, $R \in \mathbb{R}^{m \times m}$.

The system upon which the controller is evaluated is different from the system used in the controller design. The two systems can be called the *evaluation* and *design* systems, respectively. The design system is typically the evaluation system with weighted inputs and outputs. The evaluation model can be expressed in the standard system notation by first defining the output vector, z , and the disturbance vector, w , used in [12]. Let

$$w(t) = \begin{bmatrix} \xi(t) \\ \theta(t) \end{bmatrix} \quad z(t) = \begin{bmatrix} x(t) \\ u(t) \end{bmatrix} \quad (44)$$

The evaluation system can now be written

$$G_{eval} = \left[\begin{array}{c|c|c} A & \begin{bmatrix} L & 0 \end{bmatrix} & B \\ \hline \begin{bmatrix} I \\ 0 \end{bmatrix} & \begin{bmatrix} 0 & 0 \\ 0 & 0 \end{bmatrix} & \begin{bmatrix} 0 \\ I \end{bmatrix} \\ \hline C & \begin{bmatrix} 0 & I \end{bmatrix} & 0 \end{array} \right] \quad (45)$$

To derive the design model, the relative magnitudes of the input disturbances and output variables are explicitly weighted using the noise intensities, Ξ and Θ , and the output weights, Q and R , used in the quadratic cost, (43). The design plant has the form:

$$G_{des} = \left[\begin{array}{c|c|c} A & \begin{bmatrix} L\Xi^{1/2} & 0 \end{bmatrix} & B \\ \hline \begin{bmatrix} Q^{1/2} \\ 0 \end{bmatrix} & \begin{bmatrix} 0 & 0 \\ 0 & 0 \end{bmatrix} & \begin{bmatrix} 0 \\ R^{1/2} \end{bmatrix} \\ \hline C & \begin{bmatrix} 0 & \Theta^{1/2} \end{bmatrix} & 0 \end{array} \right] \quad (46)$$

Given this definition of the design plant, the \mathcal{H}_2 -norm of the design system is equivalent to the quadratic cost; that is

$$\|G_{des}\|_2^2 = J_{LQG} \quad (47)$$

and thus the problems of finding the compensator, G_c , to minimize either the average \mathcal{H}_2 -norm of the design plant or the average quadratic cost defined in (43) are equivalent.

6.2 The Robust-Control Benchmark Problem

In this section, dynamic output feedback compensators based on the techniques presented in the preceding sections will be designed for the robust-control benchmark problem presented in Ref. [18]. The problem considered is a two-mass/spring system shown in Figure 2, which is a generic model of an uncertain dynamic system with a noncolocated sensor and actuator. The uncertainty stems from an

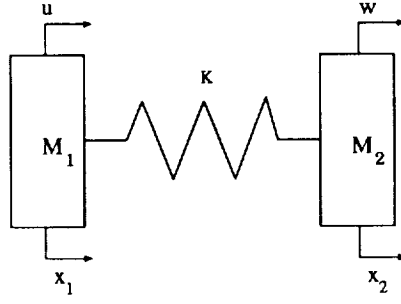


Figure 2: The Robust-Control Benchmark Problem

uncertain spring connecting the two masses. From Ref. [18] the system matrices can be represented in state space form using the notation presented in Section 6.1 as

$$A = \begin{bmatrix} 0 & 0 & 1 & 0 \\ 0 & 0 & 0 & 1 \\ -k/m_1 & k/m_1 & 0 & 0 \\ k/m_2 & -k/m_2 & 0 & 0 \end{bmatrix} \quad B = \begin{bmatrix} 0 \\ 0 \\ 1/m_1 \\ 0 \end{bmatrix} \quad L = \begin{bmatrix} 0 \\ 0 \\ 0 \\ 1/m_2 \end{bmatrix} \quad (48)$$

$$C = \begin{bmatrix} 0 & 1 & 0 & 0 \end{bmatrix} \quad (49)$$

Within the system described in Eqs. (48)-(49), the uncertain spring, k , is decomposed into a nominal value and a bounded variable parameter

$$k = k_0 + \tilde{k}, \quad k_0 = 1.25, \quad |\tilde{k}| \leq \delta_k = 0.75 \quad (50)$$

Thus the parameter design bound, $\delta_k = 0.75$, allows the stiffness to vary in the range from 0.5 to 2. With this factorization the set of systems can be defined in the notation given for the structured set of systems, Eq. 11. In particular, only the A matrix is uncertain. It can be factored as

$$A(\tilde{k}, \tilde{c}) = A_0 + \tilde{k}A_k \quad (51)$$

$$A_0 = \begin{bmatrix} 0 & 0 & 1 & 0 \\ 0 & 0 & 0 & 1 \\ -1.25 & 1.25 & 0 & 0 \\ 1.25 & -1.25 & 0 & 0 \end{bmatrix} \quad A_k = \begin{bmatrix} 0 & 0 & 0 & 0 \\ 0 & 0 & 0 & 0 \\ -1 & 1 & 0 & 0 \\ 1 & -1 & 0 & 0 \end{bmatrix}$$

With this factorization, the robust control design methodologies presented in the previous sections can be applied. The LQG problem statement presented in Section 6.1 which is based on the standard LQG design weights will be adopted. In this method the designer selects the state weighting matrix, Q , the control weighting matrix, R , and the sensor and plant noise intensity matrices, Θ and Ξ , respectively. The evaluation plant is modified as in Eq. (46) to give the design plant. The control is designed on the design plant and implemented on the evaluation plant. The weighting values used in the design are

$$Q(2, 2) = 1 \quad R = 0.0005 \quad (52)$$

Thus only the position of the second mass is penalized. The control weighting was chosen to be low to examine high performance designs which meet a settling time requirement of 15 seconds as specified in Ref. [18]. In addition to the state and control penalties, the plant noise and the plant noise intensity were assumed to be

$$\Xi = 1, \quad \Theta = 0.0005 \quad (53)$$

The signal noise intensity was chosen low to give a high gain Kalman filter in the LQG design.

Figure 3 compares the closed-loop \mathcal{H}_2 -norm resulting from the various designs using $\delta_k = 0.4$ as a function of the deviation from the nominal spring constant, \tilde{k} . Thus the controllers were designed to accommodate a stiffness variation, $0.85 \leq k \leq 1.65$. Instability regions are indicated by an unbounded closed-loop \mathcal{H}_2 -norm. The LQG results clearly indicate the well-known loss of robustness associated with high-gain LQG solutions. The LQG cost curve achieves a minimum at the nominal spring constant, $k = 1.25$, but tolerates almost no lower values of k . The stability region is increased by the PEAM and BAM designs at the cost of increasing the nominal system closed-loop \mathcal{H}_2 -norm. Although both the PEAM and the BAM designs increase robustness they do not achieve stability throughout the whole design set, $-0.4 \leq \tilde{k} \leq 0.4$. Of the approximate methods, the Bourret approximation more nearly achieves stability throughout the set. The EAM design does achieve stability throughout the set as was indicated by the analysis. The cost of this stability guarantee is loss of nominal system performance.

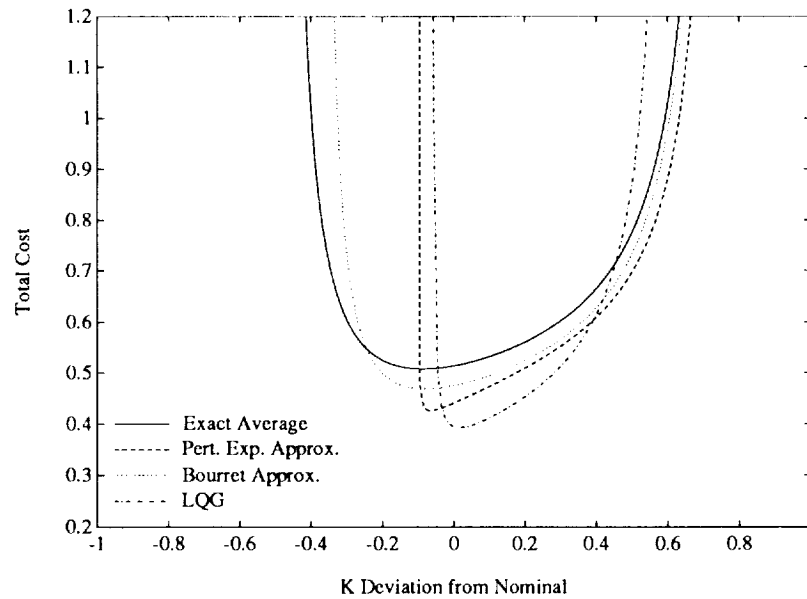


Figure 3: System Closed-Loop \mathcal{H}_2 -norm (Quadratic Cost) as a Function of the Deviation about the Nominal Spring Constant, \tilde{k} , for Controllers Designed Using $\delta_k = 0.4$.

The actual range over which a given design is stable can be plotted as a function of the parameter range used in the design. The parameter range over which a particular design maintains stability is characterized by the *achieved bound* which is chosen to be the lower limit of the stability range. The parameter range actually considered in the design is characterized by the *design bound*, denoted δ_k , which specifies the upper and lower limit of \tilde{k} . Figure 4 shows the achieved lower \tilde{k} stability bounds as a function of the design bound, δ_k . This plot is thus a measure of conservatism in the design. A conservative design would achieve stability over a much larger set of parameters actually used in its design. With no design uncertainty all five techniques converge to the stability range achieved by the standard LQG design ($|\tilde{k}| \leq 0.06$). As the uncertainty used in the design process is increased the achieved robustness is also increased. The EAM design always increases robustness enough to guarantee stability throughout the design set but the design is very nonconservative. The approximate cost minimization techniques don't provide this guarantee. The BAM design does come closer to guaranteeing stability than the PEAM design which does particularly poorly.

In Figure 5, the closed-loop \mathcal{H}_2 -norm of the nominal plant ($k = 1.25$) is examined as a function

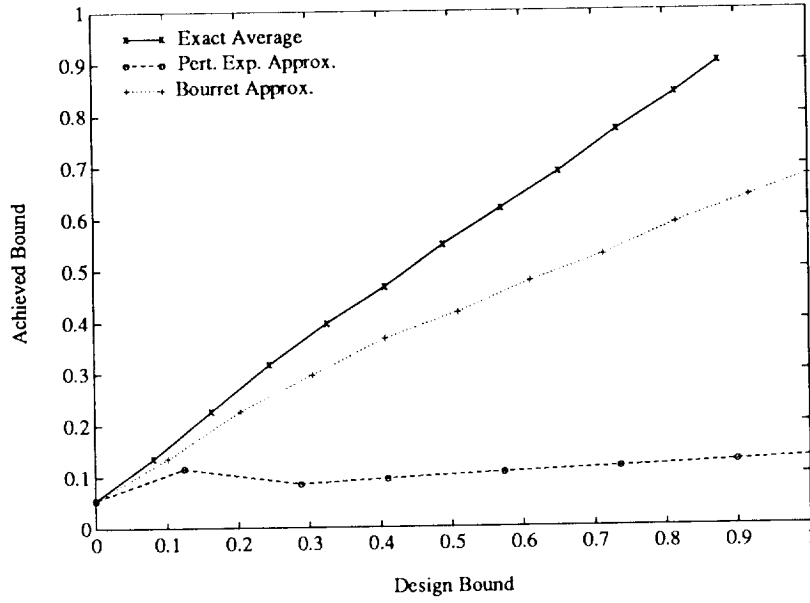


Figure 4: Achieved Closed-Loop Stability Bounds as a Function of the Design Bound, δ_k

of the achieved stability bound. A robust controller design methodology which sacrifices the least nominal performance for a given level of robustness can be called the most efficient. Figure 5 thus presents the relative efficiency of the three design techniques. The closed-loop cost (\mathcal{H}_2 -norm) is also shown decomposed into the component associated with the output weighting, called the output cost, and the component associated with the control weighting, called the control cost. The EAM design achieves a given level of robustness with the least increase in the nominal cost and is therefore considered the most efficient design. The BAM design also has good efficiency, almost matching that of the EAM design. The PEAM design is clearly the least efficient of the three. It cannot achieve a stability bound of more than 0.2.

6.3 The Cannon-Rosenthal Problem

In this section, a four mass/spring/damper problem will be examined which was presented first in [19]. The layout of the system is shown in Fig. 6. The system consists of four masses connected by springs and viscous dampers. The uncertainty enters into the problem through a variable body-1 mass. The system can be represented in state space using the notation presented in Section 6.1 as

$$A = \begin{bmatrix} 0_{4 \times 4} & I_{4 \times 4} \\ A(k) & A(c) \end{bmatrix} \quad (54)$$

$$A(x) = \begin{bmatrix} -x/m_1 & x/m_1 & 0 & 0 \\ x/m_2 & -2x/m_2 & x/m_2 & 0 \\ 0 & x/m_3 & -2x/m_3 & x/m_3 \\ 0 & 0 & x/m_4 & -x/m_4 \end{bmatrix} \quad (55)$$

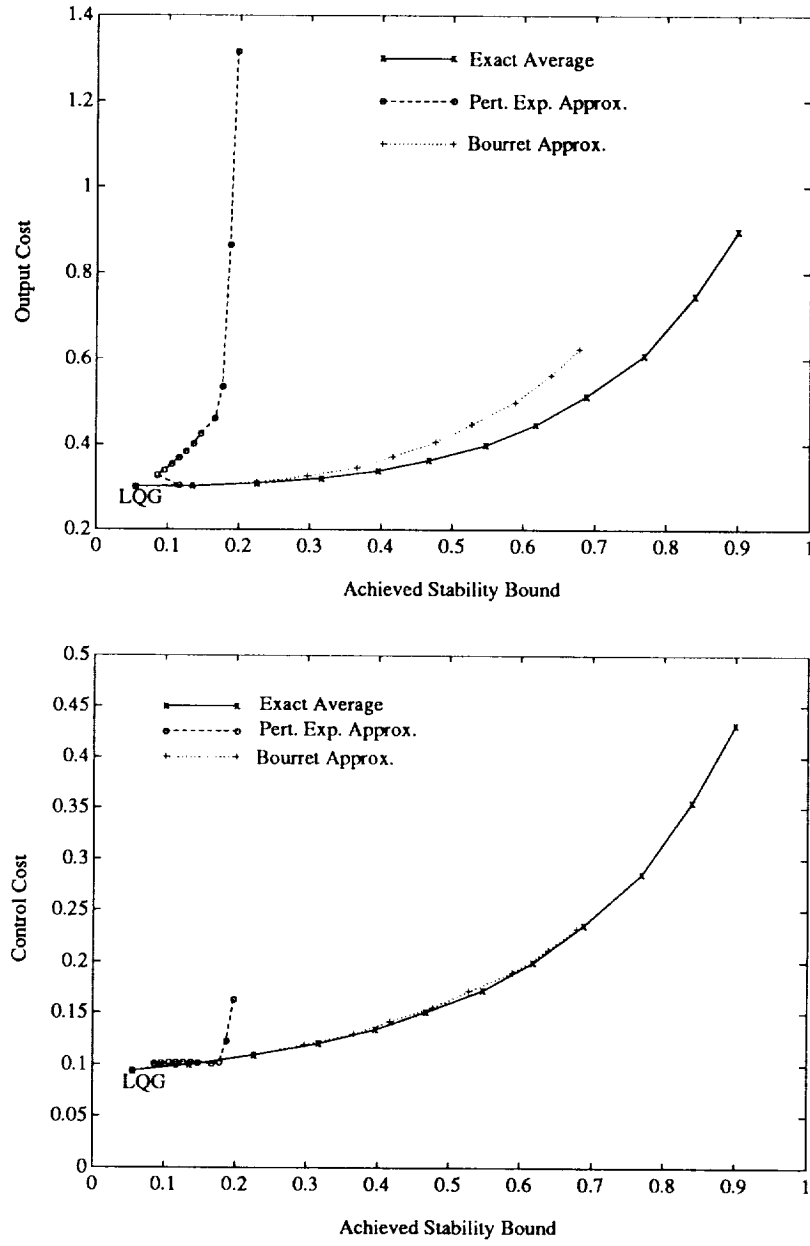


Figure 5: Output Cost and Control Cost as a Function of the Achieved Stability Bound.

$$L = \begin{bmatrix} 0 \\ 0 \\ 0 \\ 0 \\ 0 \\ 0 \\ 0 \\ 1/m_4 \end{bmatrix}, \quad B = \begin{bmatrix} 0 \\ 0 \\ 0 \\ 0 \\ 0 \\ 1/m_2 \\ 0 \\ 0 \end{bmatrix}, \quad C = [0 \ 0 \ 0 \ 1 \ 0 \ 0 \ 0 \ 0] \quad (56)$$

For this problem the nominal values of the springs, dampers and masses were chosen to be $k = 1$, $c = .01$, $m_2 = m_3 = m_4 = 1$, and $m_1 = 0.5$. Within the system described in Eqs. (54)-(56), the

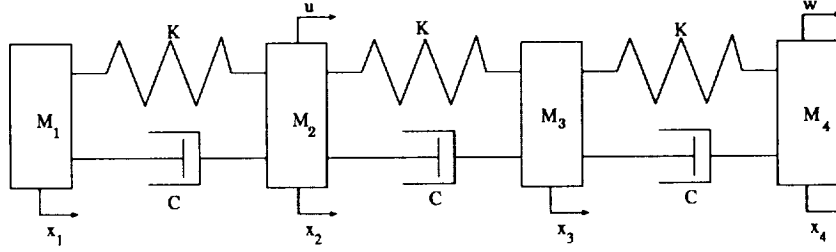


Figure 6: The Cannon-Rosenthal Problem

uncertain mass, m_1 , enters into the equations through its inverse. The inverse of the mass will therefore be used as the uncertain parameter called \tilde{m} . If the nominal value of m_1 is 0.5, then the uncertainty can be represented as

$$1/m_1 = 1/m_{10} + \tilde{m}, \quad m_{10} = 0.5, \quad |\tilde{m}| \leq \delta_m \quad (57)$$

Thus m_1 varies from 1 to 0.25 as \tilde{m} varies from -1 to 2. Only the A matrix is uncertain. It can be decomposed as

$$A(\tilde{m}) = A_0 + \tilde{m}A_m$$

in a manner analogous to the factorization for the uncertain spring in the robust-control benchmark problem. This problem was considered because of a pole-zero flip caused by the uncertain mass. In addition to changing the natural frequencies of all of the modes, as the mass is decreased from its nominal value of 0.5 to 0.25, an undamped zero between the first and second modes moves to between the second and third modes. This type of uncertainty is especially difficult to deal with since in effect the phase of the second mode can vary by ± 180 degrees between elements of the model set. This pole-zero flip makes the robust control design problem difficult. In addition if there is little damping, then the system effectively becomes uncontrollable or unobservable when the pole and zero cancel.

The robust control design methodologies presented in the previous sections can be applied to this problem. Just as in the Robust Control Benchmark Problem, the method of weighting the system that was presented in Section 6.1 which is based on the standard LQG design weights will be used for the control design. The evaluation plant given in Eqs. (54)-(56) is modified as in Eq. (46) to give the design plant. The control is designed on the design plant and implemented on the evaluation plant. Only the position of the fourth mass was penalized. The weighting values used in the design are

$$Q(4,4) = 1, \quad R = 0.05 \quad (58)$$

In addition to the state and control penalties, the plant noise and the plant noise intensity were assumed to be

$$\Xi = 1, \quad \Theta = 0.05 \quad (59)$$

This choice of penalties makes the LQG controller very sensitive to m_1 variation and thus presents a challenging robustness problem for the average-based methods.

The robustness properties of the control designs are compared to those of the standard LQG design in following discussions. Figure 7 compares the closed-loop \mathcal{H}_2 -norm resulting from the various designs using $\delta_m = 0.1$ as a function of the deviation, \tilde{m} , from the nominal system mass. Thus as \tilde{m} varies in the range, $-0.1 \leq \tilde{m} \leq 0.1$, m_1 varies in the range, $2.5 \geq m_1 \geq 1.6$. Instability regions are indicated by unbounded closed-loop \mathcal{H}_2 -norm. The designs can thus be considered stable inside the region described by the upper and lower asymptotes. These asymptotes will be called the upper and lower achieved stability bounds for the particular problem.

The LQG results clearly indicate the well-known loss of robustness associated with high-gain LQG solutions. The LQG cost curve achieves a minimum at the nominal mass value, $\tilde{m} = 0$, but tolerates almost no variation in \tilde{m} . The stability region is increased by the PEAM and BAM designs at the cost of increasing nominal system closed-loop \mathcal{H}_2 -norm. The PEAM design increases robustness, but it does not achieve stability throughout the whole design set. The Bourret approximation does achieve stability throughout the set. The EAM design also achieves stability throughout the set as was indicated by the analysis. The cost of this stability guarantee is loss of nominal system performance, although for this small amount of uncertainty the performance loss is negligible.

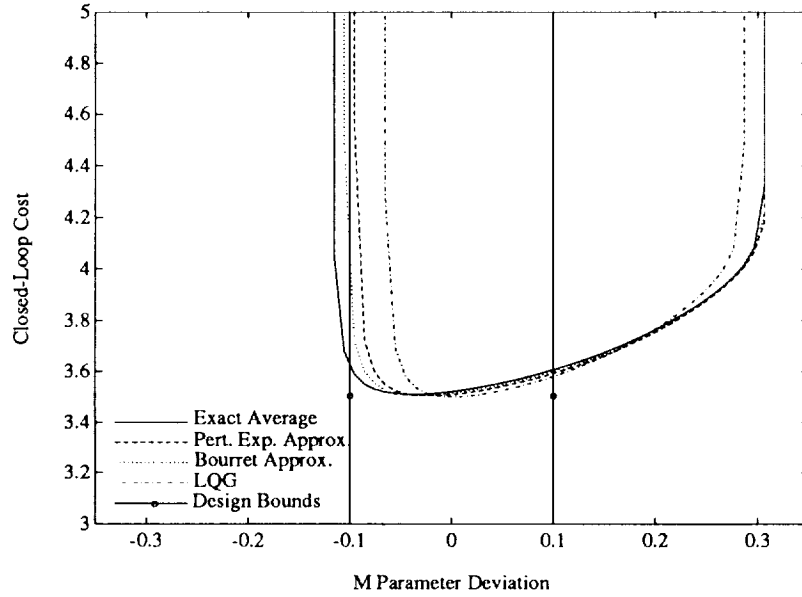


Figure 7: System Closed-Loop \mathcal{H}_2 -norm as a Function of \tilde{m} , the Deviation about $1/m_1$, for Controllers Designed Using $\delta_m = 0.1$.

Figure 8 shows the lower values of \tilde{m} beyond which the respective designs are unstable as a function of the bound on the parameter variation used in the design, δ_m . Figure 8 is thus a plot of the actual stability range achieved as a function of the parameter bound used in the design. The system is thus stable in the range

$$-\delta_a \leq \tilde{m} \leq \delta_a$$

where δ_a is the achieved lower stability bound. For the designs considered, the lower \tilde{m} bound was always smaller than the upper indicating that the design procedures had more difficulty extending the stability range for negative \tilde{m} (large mass) than for positive \tilde{m} (smaller mass).

With no design uncertainty all five techniques converge to the stability bounds achieved by the standard LQG design ($|\tilde{m}| \leq 0.06$). Just as for the Robust-Control Benchmark Problem, as the uncertainty used in the design process is increased the achieved robustness is also increased. Again, the EAM design always increases robustness enough to guarantee stability throughout the design set, while the approximate cost minimization techniques don't provide this guarantee. Their curves lie below that of the EAM design. The EAM design curve has unity slope indicating that the EAM design achieves extremely nonconservative stability over the parameter set used in the design as was predicted by the analysis. The BAM design does come closer to guaranteeing stability than the PEAM design which has difficulty extending the stability range. In particular, for the PEAM design, increasing the design bound above $\delta_m = 0.5$ yields no increase in the achieved stability bound.

The design costs associated with the nominal system ($\tilde{m} = 0$) are plotted as a function of the

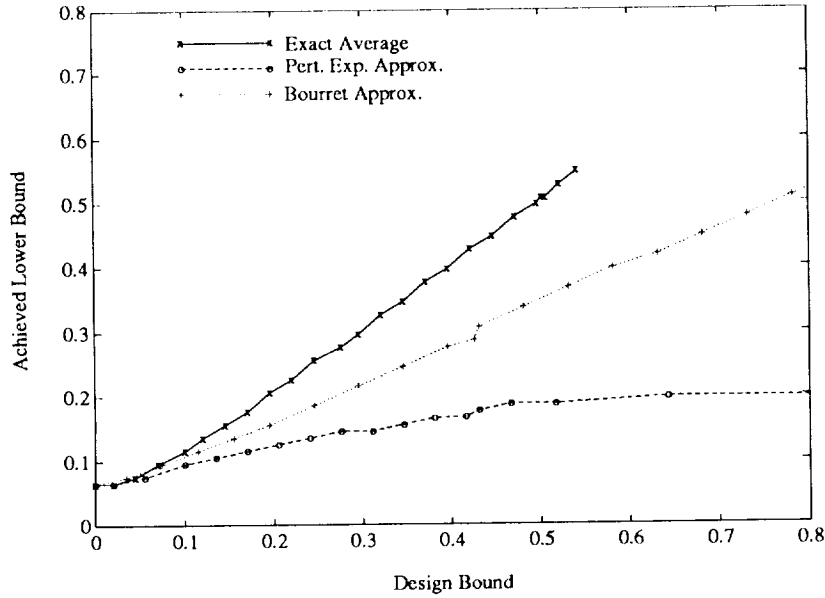


Figure 8: Achieved Lower Closed-Loop Stability Bounds as a Function of the Bound Used in the Design, δ_m .

achieved lower stability bound in Figure 9. Figure 9 is an indicator of the design efficiency of the robust design procedure. The EAM design is most efficient followed by the BAM design. In this problem the PEAM design exhibited much better relative efficiency than in the previous section. It cannot however yield controllers with stability bounds larger than 0.2. Increasing the design bound has no effect on the achieved bound. In essence the EAM design “stalls” out. This is possible because there are no stability guarantees associated with a given design bound.

The output costs are the chief contributors to the total cost as shown in Fig. 9. The control cost shown in Fig. 9 is lowered in all of the designs methods so as to increase the achieved stability robustness. Lowering the control cost is indicative of lower gain controllers. This is the opposite trend as the one observed in the benchmark problem where the control cost increased with greater achieved stability range. For the Cannon-Rosenthal Problem there are modes which cannot be phase stabilized due to the large phase uncertainty caused by the pole-zero flip. The only alternative left to the robust design procedure is gain stabilization as was employed.

7 Experimental Implementation

In this section, experiments on robust control of an optical pathlength on the MIT multipoint alignment testbed will be presented. The testbed was designed as a technology demonstrator for active control of precision structures with particular emphasis on technology necessary for very large baseline optical interferometry. In consideration of this purpose the stabilization of an optical pathlength using an active member within the structure was chosen as a characteristic problem. Detailed descriptions of the testbed hardware including the active member actuators, laser metrology systems, and real time control computer are available in Ref. [20] and will not be presented here. The particular problem considered is an SISO control loop from an active member located behind siderostat A to optical pathlength from siderostat A to the vertex at F, as shown in Figure 10. The problem is noncollocated and particularly difficult due to the inaccuracies of the model used for control design.

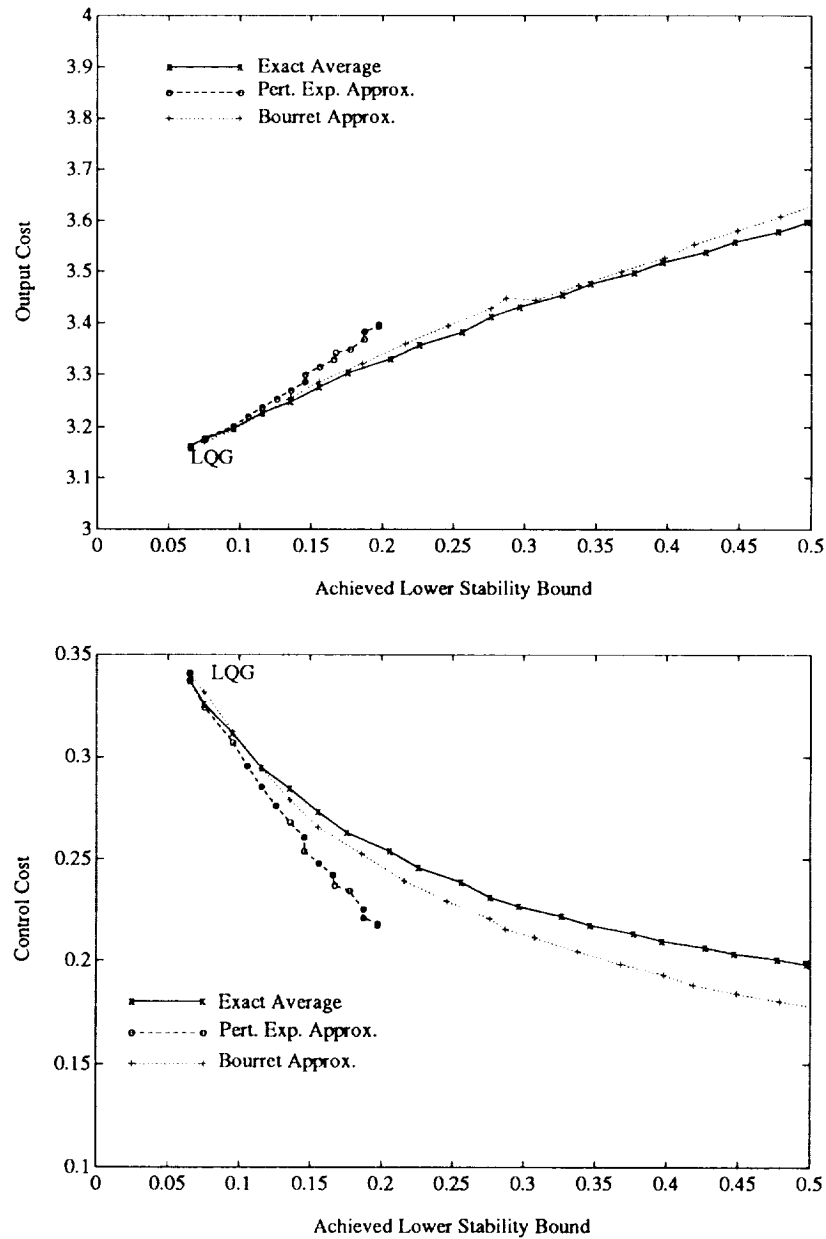


Figure 9: Output Cost and Control Cost as a Function of the Achieved Stability Bound.

All controllers designed in this section are based exclusively on the finite element model of the test-bed with the exception of DC gain information. The intent is to compare the achievable performance of an LQG compensator designed using the inaccurate model with that of a cost-averaging based compensator designed with explicit treatment of the model uncertainty. A comparison of the FEM and the measured transfer functions is shown in Figure 11. The modal frequencies of the FEM are an average of 5-10% in error and the damping ratios are as much as 100% in error. More importantly the modal residues and relative controllability and observability of the modes are in error especially in the region above 50 Hz. The plot of the magnitude of the error transfer function is shown in Figure 12. The additive error exceeds one at almost every mode. Small gain theory measures of robustness would require a compensator to roll-off significantly before the first mode. In addition to the modal

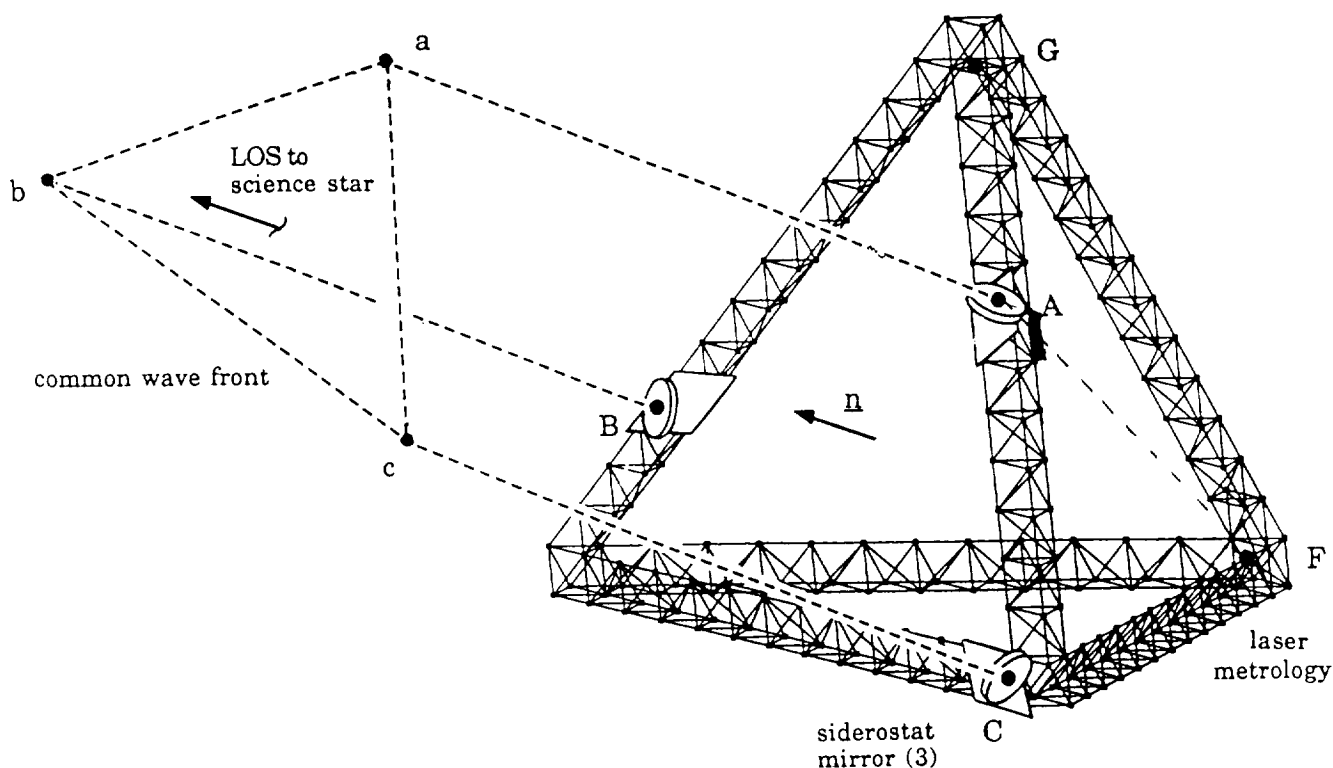


Figure 10: Schematic of the MIT multipoint alignment testbed showing controller optical path (A-F) and the active member control actuator (A).

errors there is phase drift caused by mismodelled time delay associated with the real time control computer.

The finite element model has 45 modes in the range from 0.3 (suspension) to 159.7 Hz. It was necessary to reduce the size of the model for control design. Initially, the model was truncated to retain only the 20 modes in the 10-100 Hz range. The model was further reduced by truncating a balanced realization of the system to the desired order. The controllers were then derived using the reduced system model. Initial experience with LQG controllers penalizing pathlength and control showed that there was no difference in achievable experimental performance when using either a 22 order compensator designed from the reduced FEM or a fourth order compensator designed from a further reduced model. The large uncertainties between the model and the plant limited performance to a gain level below that at which the compensator order effects became important. This fact, coupled with the severe model size limitations imposed by the computation of the averaged-cost based controllers, leads to the selection of a fourth order design plant shown in Figure 13. A mode was retained in the design model at 56 Hz to represent dynamics in the critical region of model uncertainty, those modes from 50-70 Hz.

Two types of controllers were designed and compared based on the fourth order design plant. The first was a LQG based design penalizing optical pathlength error as well as active member control voltage. The plant disturbance entered at the actuator, and the sensor noise entered in the optical pathlength. The pathlength error penalty and disturbance magnitude were normalized to unity while the effective compensator gain was changed by varying the control penalty and sensor noise intensity together. There is thus only a single variable weight used to generate the family of compensators presented.

In the LQG design the mode at 56 Hz was considered certain. In the average cost based design,

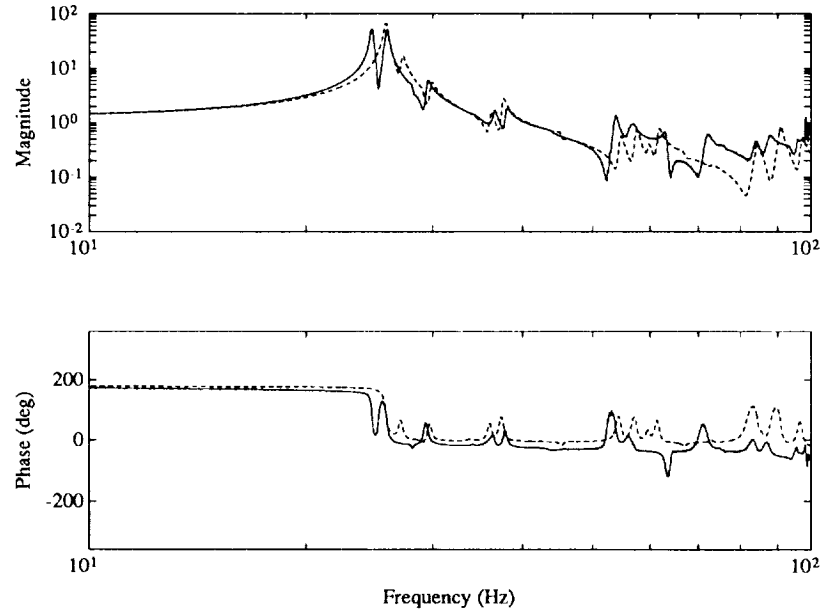


Figure 11: Magnitude and Phase of the Measured Transfer Function from Active Strut to Optical Pathlength (solid) to that Derived from the FEM (dashed).

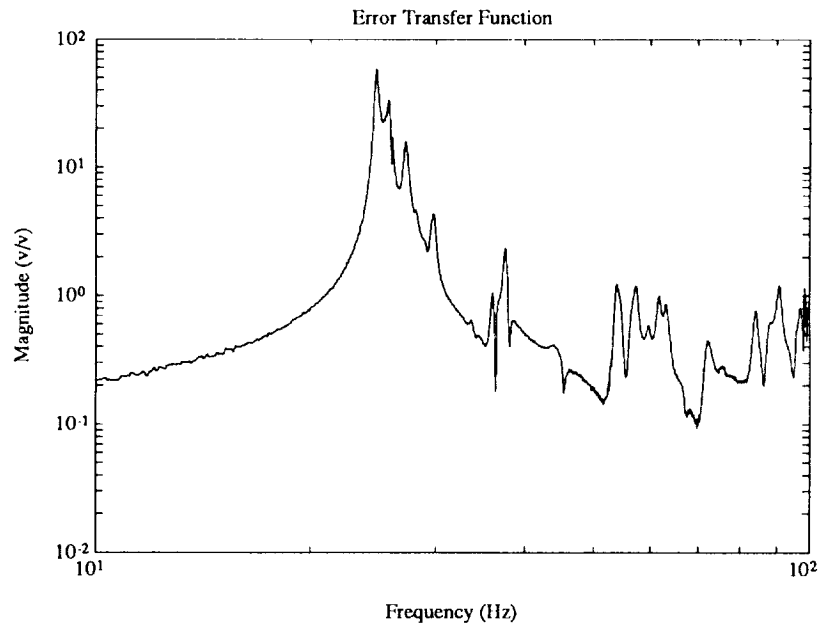


Figure 12: Magnitude of the Additive Error Between the Measured Plant Transfer Function and the FEM Derived Transfer Function.

this mode was assumed to have an uncertain natural frequency varying in the range of $\pm 30\%$ about the nominal. It was hoped that this natural frequency uncertainty would discourage the compensator from plant inversion in the highly uncertain region from 50-70 Hz. The Bourret approximate average cost design technique was chosen because of its superior performance in the analytical sample problems. The weightings used in the Bourret cost minimization were identical to those used in the LQG

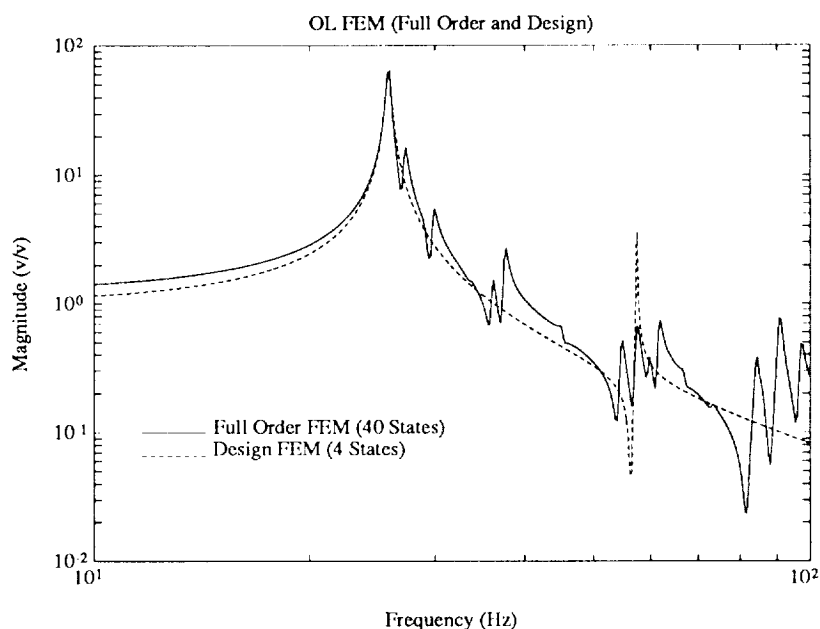


Figure 13: Magnitude of Full Order FEM compared to Fourth Order Design Model

problem.

The closed loop results for compensators based on the two design methods (LQG and Bourret) are presented in Figures 14 - 15. Figure 14 presents the tradeoff between achieved performance and controller effort expended. The performance is a measure of the rms pathlength error nondimensionalized by the open loop rms in the frequency range from 10-100 hz. The control effort is the rms control signal normalized by this same quantity. There is a clear performance improvement with the use of active control. As more control effort is expended, the rms pathlength error can be decreased to only 25% of its open loop value before the onset of instability. The achieved performance-control effort trade eventually diverges at high gain from that predicted when applying the compensators to the full order FEM. This divergence occurs when either controller has a bandwidth which encroaches on the highly uncertain modes in the range from 50-70 hz.

Both the LQG and the Bourret controllers go unstable at approximately the same level of gain. The best achieved experimental closed loops for the two controllers are shown in Figure 15. The robust controller was not able to add significantly to the achievable performance using the assumed single-mode uncertainty structure. As shown in Figure 15, it did change the actual mode which first goes unstable from one at 52 hz to one at 56 hz. Figure 16 shows the predicted performance of the compensators (LQG and Bourret) on the full order FEM. In contrast with the actual system, the modes from 50-70 hz in the FEM do not interact unstably with either compensator.

The poor modelling of the modes in the 50-70 hz region may require the use of multiple uncertain modes in the compensator design rather than the single mode used in the present robust control design. Since the present implementation of the Bourret controller design method is computationally intensive, these designs are effectively limited to accommodate only a few (1-3) uncertainties and a few modes. Practical application to this problem will require improved controller computational methods (more computer power) and/or better methods for selecting which uncertain modes and parameters should be retained in the design.

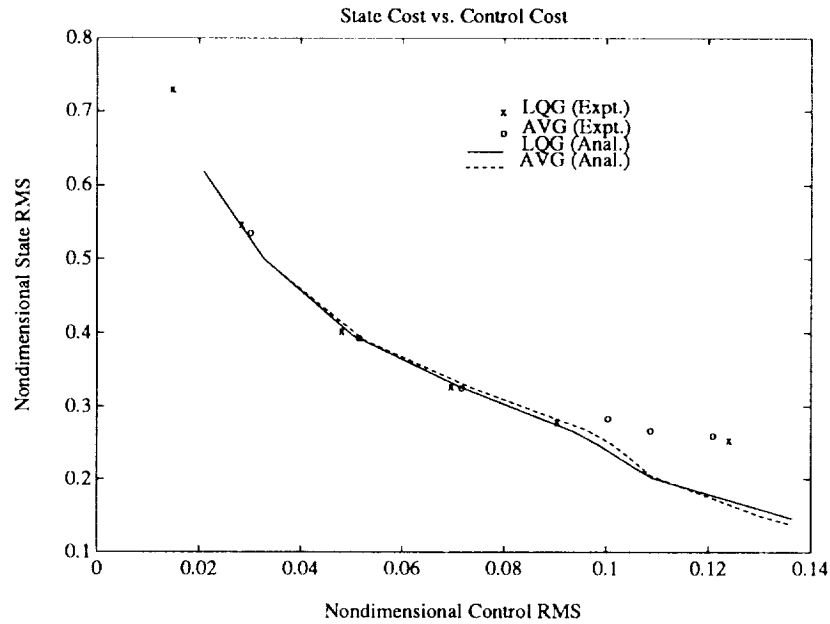


Figure 14: Nondimensional Closed Loop RMS Pathlength Error as a Function of the Nondimensional Control Effort.

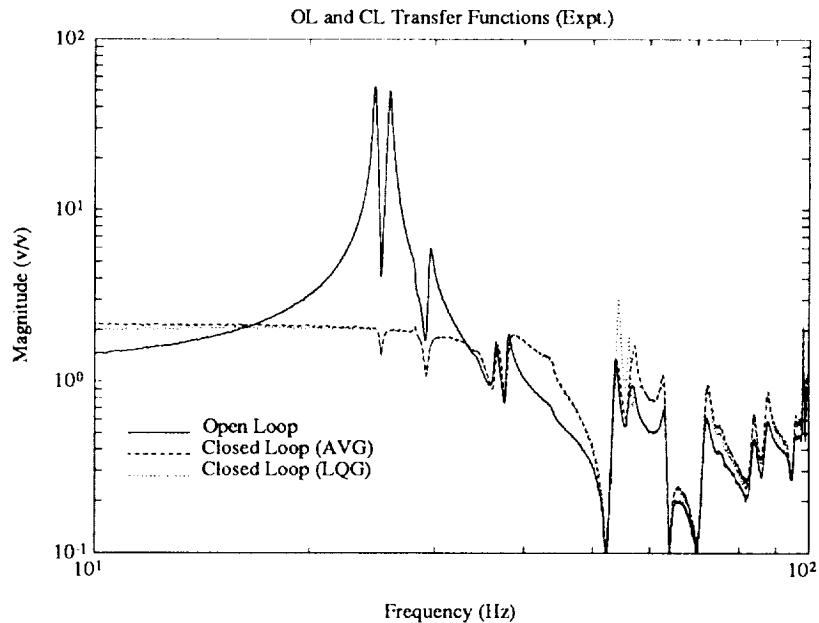


Figure 15: Experimental Open Loop (solid), Bourret Approximate Average Closed Loop (dashed), and LQG Closed Loop (dotted) Transfer Functions

8 Summary and Conclusions

The problem of computing the exact and approximate average \mathcal{H}_2 -norm of a linear time invariant system has been addressed. This was motivated by showing that bounded average \mathcal{H}_2 -norm implies stability throughout the model set. Therefore minimization of the average cost will guarantee stability

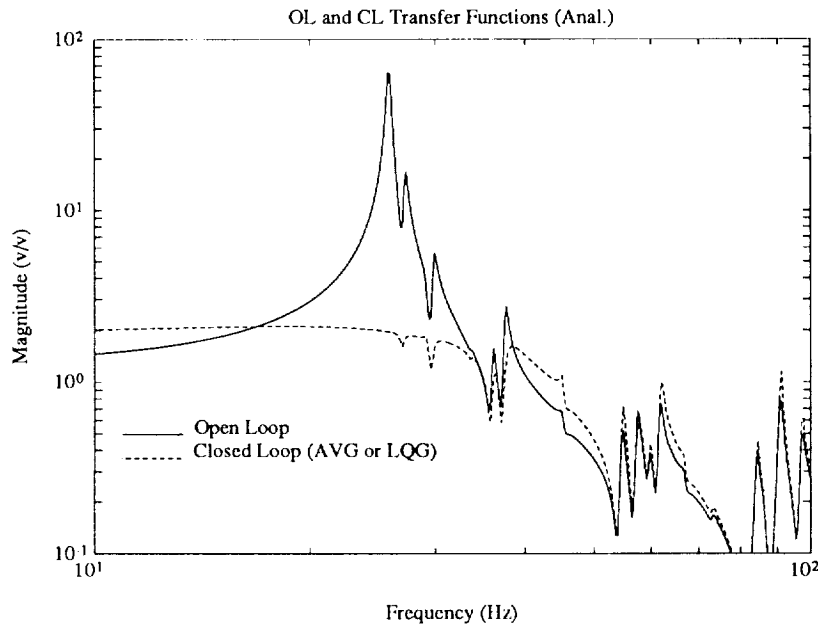


Figure 16: FEM based Analytical Open Loop (solid), Bourret Approximate Average Closed Loop (dashed), and LQG Closed Loop (dotted) Transfer Functions

without having to resort to worst case design techniques. Because the exact average cost is essentially uncomputable, two approximations were applied to the problem. The first approximation is based off of a perturbation expansion about the nominal Lyapunov equation solution, while the second is based on a more sophisticated technique widely used in the field of random wave propagation and turbulence modelling. Using these approximations, cost functionals were derived which are not parameterized and therefore suitable for control synthesis.

The average performance problem was formulated for dynamic output feedback. The cost minimized was represented by either the exact average, the perturbation expansion approximation, or the Bourret approximation to the average. Each cost minimization yields different necessary conditions and different properties for the resulting controllers. When the exact average cost is minimized they yield controllers which guarantee stability throughout the model set. Minimizing the approximations to the average increased robustness over the non-augmented cost minimization, (LQG), but did not necessarily guarantee stability throughout the model set. The numerical examples indicated that the Bourret approximation produced controllers whose properties more closely approximated those of the exact average based controllers. The Bourret approximate average minimization also resulted in less cost increase for a given stability range and can thus be considered a more efficient design methodology than the perturbation approximation minimization.

The experimental application of the method to pathlength control on the MIT multipoint alignment testbed revealed some weaknesses in the techniques. The controllers were calculated using an iterative parameter optimization which was computationally intensive. The difficulties in controller calculation presently limit the methods applicability to robust control on large order systems with many uncertain parameters. The methods could however be profitably applied to the problem of uncertain model reduction where the computation requirements are not as great. Further work is underway in the area of uncertain model reduction and selection of appropriate uncertain parameters for retention in control design.

References

- [1] Ashkenazi, A. and Bryson, A. E., "Control Logic for Parameter Insensitivity and Disturbance Attenuation," *AIAA J. of Guidance and Control*, Vol. 5, No. 4, 1982, pp. 383-388.
- [2] Miyazawa, Y., "Robust Flight Control System Design with the Multiple Model Approach," *Proc. AIAA Guid. Nav. Contr. Conf.*, Portland OR, Aug. 1990, pp. 874-882.
- [3] Gangsaas, D., Bruce, K. R., Blight, J. D., and Ly, U. "Application of Modern Synthesis to Aircraft Control," *IEEE Trans. Autom. Contr.*, Vol. AC-31, No. 11, Nov. 1986, pp. 995-1014.
- [4] R. Saeks and J. J. Murray, "Fractional representation, algebraic geometry and the simultaneous stabilization problem," *IEEE Trans. Autom. Contr.*, Vol. AC-27, No. 4, Aug. 1982, pp. 895-903.
- [5] B. K. Ghosh and C. I. Byrnes, "Simultaneous stabilization and simultaneous pole placement by non-switching dynamic compensation," *IEEE Trans. Autom. Contr.*, Vol. AC-28, No. 6, June 1983, pp. 735-741.
- [6] P. M. Makila, "On multiple criteria stationary linear quadratic control," *IEEE Trans. Autom. Contr.*, Vol. 34, No. 12, Dec. 1989, pp. 1311-1313.
- [7] D. MacMartin, S. R. Hall, and D. S. Bernstein, "Fixed order Multi-Model Estimation and Control," Presented at the 1991 ACC Conference.
- [8] Hopkins, W. E. Jr., "Optimal Control of Linear Systems with Parameter Uncertainty," *IEEE Trans. Autom. Contr.*, Vol. AC-31, No. 1, January 1986, pp. 72-74.
- [9] Hagood, N. W., *Cost Averaging Techniques for Robust Control of Parametrically Uncertain Systems*, Phd Thesis, Massachusetts Institute of Technology, Department of Aeronautics and Astronautics, June 1991.
- [10] Hagood, N. W., "Cost Averaging Techniques for Robust Control of Parametrically Uncertain Systems," Presented at the 1991 AIAA Guidance Navigation and Control Conference, New Orleans,
- [11] Hyland, D. C., and Bernstein, D. S., "The Optimal Projection Equations for Fixed-Order Dynamic Compensation," *IEEE Trans. Auto. Contr.*, Vol. AC-29, No. 11, Nov. 1985, pp. 1034-1037.
- [12] Doyle, J. C., Glover, K., Khargonekar, P. P., Francis, B. A., "State Space Solutions to Standard \mathcal{H}_2 and \mathcal{H}_∞ Control Problems" *IEEE Trans. Autom. Contr.*, Vol. AC-34, No. 8, August 1989, pp. 831-847.
- [13] Frisch, U. "Wave Propagation in Random Media" *Probabilistic Methods in Applied Mathematics* Vol. 1, Edt. A. T. Bharuch-Reid, Academic Press, NY, 1968 ,pp 75-197.
- [14] Yedavalli, R. K., and Skelton, R. E., "Determination of Critical Parameters in Large Flexible Space Structures with Uncertain Modal Data," *Journal of Dynamic Systems, Measurement, and Control*, Vol. 105, December 1983, pp. 238-244.
- [15] Athans, M., "The Matrix Minimum Principle," *Inf. and Cntrl.* Vol. 11, 1968, pp. 592-606.
- [16] Okada, K., Skelton, R. E., "Sensitivity Controller for Uncertain Systems," *AIAA Journal of Guidance, Control and Dynamics*, Vol. 13, No. 2, March-April 1990, pp. 321-329.
- [17] Wie, B., and Bernstein, D. S., "Benchmark Problems for Robust Control Design," *Proc. 1991 ACC Conf.*, June, 1991.
- [18] Cannon, R. H., Rosenthal, D. E., "Experiments in Control of Flexible Structures with Non-colocated Sensors and Actuators," *AIAA Journal of Guidance, Control, and Dynamics*, Vol. 7, No. 5, Sept.-Oct. 1984, pp. 546-553.
- [19] Blackwood, G. H., Jacques, R. N., and Miller, D. W., "The MIT multipoint alignment testbed: technology development for optical interferometry," Presented at the SPIE Conference on Active and Adaptive Optical Systems, San Diego, CA 22-25 July, 1991 SPIE paper No. 1542-34.